Impact of Failure-surface Parameters of Concrete Damage Plasticity Model on the Behavior of Reinforced Ultra-high Performance Concrete Beams

Adil M. Jabbar[1*]

[1] Civil Engineering Department, College of Engineering, Wasit University, Wasit, 52001, Al Kut, Iraq
* Corresponding author, e-mail: adilmahdi@uowasit.edu.iq

Abstract

The failure surface of elements can numerically represent by a concrete damage plasticity (CDP) model in Abaqus software which depends on five parameters. The parameters are eccentricity, shape, biaxial to uniaxial compressive strength ratio, dilation angle, and viscosity. This paper studies the effect of changing the values of the failure surface parameters on the bearing capacity, deflection, and overall structural behavior of ultra-high performance concrete (UHPC) beams. The parameters' changes include reasonable values higher or lower than the values adopted by Abaqus. An experimentally performed reinforced UHPC beam is simulated by Abaqus, and the five parameters are calibrated to coincide with the practical results. Then, one of the parameters is changed while others remain constant for each alteration to study its effect on the UHPC beam behavior. The numerical analysis results show that all five parameters do not affect the loading capacity and the corresponding deflection at the first cracking state. At peak state, the eccentricity does not affect the load and deflection. The influence of shape and the biaxial to uniaxial compressive strength ratio are confined to the deflection at peak load only without affecting the bearing capacity. The dilation angle effect appears when it is greater than 30 degrees to 56 degrees, while when it is less than 30, it does not affect the load and deflection. Rising the dilation angle and viscosity value promotes the peak load and the deflection.

Keywords

Abaqus, concrete damage plasticity model, dilation angle, shape parameter, viscosity, eccentricity

1 Introduction

Structural analysis software is considered a preferred method for evaluating the requirements for designing and analyzing the structural elements of complex and simple facilities. On the other hand, high construction costs often necessitate the analysis of structural members using expert software [1]. Abaqus is a specified structural analysis program using the finite element (FE) method. It can be used to simulate the linear and nonlinear behavior of reinforced concrete members by using concepts of isotropic elastic damage in linear behavior, besides isotropic plastic compressive and tensile behavior for the inelastic state [2–4]. Simulation of structural members by Abaqus consists of several steps, starting with drawing the parts, modeling the materials' properties, and erecting and defining the sections. Then these parts are assembled to form the structural member. Other steps are required to complete the analysis accurately, like the interaction between the constituents of the member, constraint, seeding of the member parts, loading, and finally, running the analysis process to attain the results by visualization step.

Modeling of materials' properties is one of the most significant steps that impact the behavior of reinforced concrete members upon loading and managing the load capacity, deflection, and crack pattern. The property step includes material behavior in the elastic and plastic stages upon loading. The elastic behavior of concrete can be defined by elastic modulus and Poisson's ratio. For inelastic, the Abaqus library contains three models to simulate the plastic behavior of concrete. These models are concrete damage plasticity (CDP), concrete smeared cracking (CSC), and brittle cracking [3, 4]. The last two models are connected to the brittle fracture concept. The CDP model is usually used to simulate the plastic behavior of concrete since it contains the most pivotal and significant

features for quasi-brittle materials [5, 6]. The CDP model can deal with the transformation of strain energy from an elastic to an elastoplastic state and finally arrive at a fully plastic state [7]. Defining the plastic behavior of concrete by the CDP model requires defining three sets of numerical data related to the concrete properties. The first set represents the concrete compression behavior, which can be defined by yielding stresses and the affiliated inelastic strains. The second set is tensile behavior after cracking by introducing cracking stresses versus cracking strains. Corresponding compression and tension damage parameters can also be defined in concurrence with the compressive and tensile behavior. Ibrahim and Rad [8, 9] derived expressions to define the isotropic elastic damage and isotropic tensile and compressive plasticity depending on the failure process of tensile cracking and compressive crushing. The third set assigns the failure surface of concrete elements and is defined by five parameters. These parameters are dilation angle (ψ), the proportion between initial biaxial compressive strength to the uniaxial one (f_{bo}/f_{co}), eccentricity (ε), the shape parameter (K) which represents the proportion between the second tensile stress to that of compression, and the viscosity parameter (μ) [4–6, 10, 11].

Abaqus software can analyze linear and nonlinear geometry of finite elements [4, 5] depending on materials' modeling to reflect its behavior on the beam behavior upon loading since beam behavior is a repercussion of the behavior of its components.

Ultra-high performance concrete (UHPC) differs from normal and high-strength concrete by its high strength and ductile behavior after cracking. UHPC is a cement-based composite material. It consists of high cement content, fine silica fume, fine and ultra-fine aggregate, low water to cementitious materials (w/cm) ratio, ignoring coarse aggregate, and a high dosage of high range water reducing admixture (HRWRA). Those constituents improve the backing density of the composite and reduce the porosity. Therefore, they increase the compressive strength to about 150 MPa. UHPC also contains steel fibers. Incorporating steel fibers through the matrix of UHPC acts as a micro reinforcement to improve ductility and tensile strength and enhance strain softening after cracking in tension and after fracture in compression [12]. Simulation of these features by Abaqus requires suitable modeling for materials in compression and tension, besides calibration of the failure surface parameters.

This paper introduces the effect of changing the values of the five parameters that define the failure surface on the behavior of the reinforced UHPC beams in terms of bearing capacity, deflection, failure type, and cracking pattern. For this purpose, a practically implemented reinforced UHPC beam is represented by Abaqus software, where the five parameters are calibrated to correspond to the practical results. Then, one of the parameters is changed while others remain constant for each modification to study its effect on the UHPC beam behavior.

2 Defining the parameters of the surface failure

The definition of failure surface parameters is based on some notions and concepts that have been evolved by scientists to explain the concrete attitude upon loading until failure.

2.1 Shape parameter (K)

The fracture shape of the element surface in the CDP model represents a modification of Drucker-Prager's strength supposition for principal stresses, where the fracture surface at plane stress is not circular but deviates inward [13, 14], as shown in Fig. 1. The nonlinear fracture surface is governed by a shape parameter to represent the failure shape (K). It is physically defined as the proportion between the second tension to second compression stress on the same hydrostatic pressure at initial fracturing at any variation in pressure, such that the maximum principal stress is negative [13, 15–17]. K-value ranges between (0.5–1.0). Abaqus adopted 2/3 as a default value for the shape parameter [4].

Most researchers; Chen and Graybeal [5], Solhmirzae and Kodur [6], Bahij et al. [18], Zhang et al. [19], Rossi et al. [20], Hashim et al. [21], adopted a 2/3 value for K in exemplifying the fracture surface of the UHPC. Othman
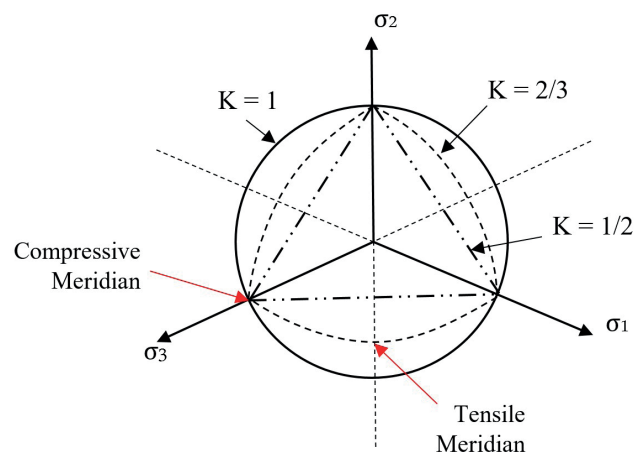

Fig. 1 Yield surfaces in the deviatory plane ($K = 2/3$ corresponding to Rankine formulation and $K = 1$ corresponding to Drucker-Prager criterion)

and Marzouk [15] showed that the multiaxial test clarified that the distorted surface of UHPC was approaching a circular shape at an elevated pressure, which means the *K*-value arrived at 1.0. In this study, three values for *K* are tested.

2.2 Dilation angle (ψ)

The dilation refers to a volume change caused by compression. It represents a physical property and is commonly used to express the deformation in soils and sands when compressed. However, it is identified as an essential component of the stress-strain behavior of granular materials. For concrete behavior in Abaqus, the dilation angle represents the element deviation when it undergoes the induced stress, as shown in Fig. 2.

The dilation angle also assigns the tendency of the fracture surface in the semi-conical form of stress transit [17], as illustrated in Fig. 3. Therefore, it controls the volumetric strain when plastic deformation occurs, which means the volumetric strain that develops in concrete particles when subject to shear deformation. Many researchers adopted (25–50) degrees as a value for the dilation angle, while Chen and Graybeal [5] used 15 degrees for UHPC.
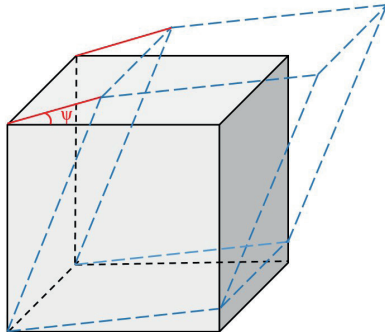

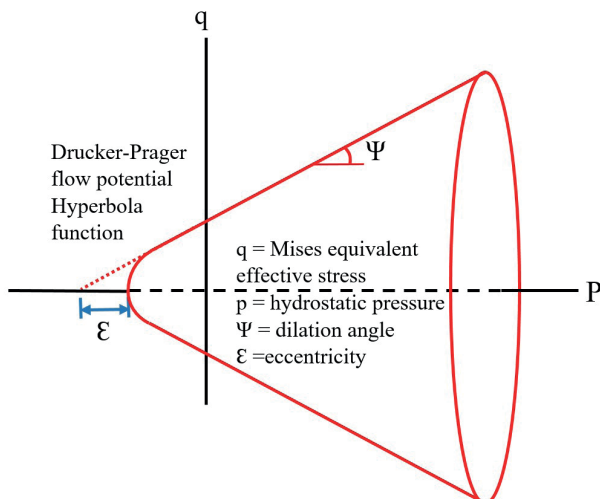**Fig. 2** The deviation of an element and the dilation angle created

Fig. 3 Dilation angle and eccentricity from the meridian plane [3]

Wosatko et al. [17] showed that increasing the dilation angle value from 5 to 55 degrees causes raising the load capacity by more than 114% while increasing it from 5 to 35 raises the load capacity by 79%.

In this study, several values for the dilation angle are tested to identify its effect on the behavior of UHPC beams consistent with the other parameters.

2.3 The Proportion between biaxial and uniaxial compressive strength (f_{bo}/f_{co})

This parameter characterizes the state of concrete when subjected to biaxial stress. Abaqus software adopts the biaxial model developed by Kupfer [13] to define the surface failure of concrete upon being subjected to biaxial compressive stresses [22, 23], as shown in Fig. 4. Abaqus adopted 1.16 as a default value. Kupfer stated that the concrete strength under biaxial compression is higher than that under uniaxial compression by only 16%, whereas the biaxial tensile strength is approximately equal to its uniaxial tensile strength [11, 24].

2.4 Eccentricity (ε)

The eccentricity represents the flow function rate of the failure cone approaches the asymptote. It relates to the dilation angle, as shown in Fig. 3 [4, 14]. Abaqus adopted 0.1 as a default value [4].

2.5 The Viscosity Parameter (μ)

The last parameter adopted by Abaqus to complete the definition of the CDP is viscosity (μ). It represents the fracture fashion or the stiffening style of the substance after maximum tolerance. Therefore, it explains the concrete behavior when transforming from not cracked to a cracked
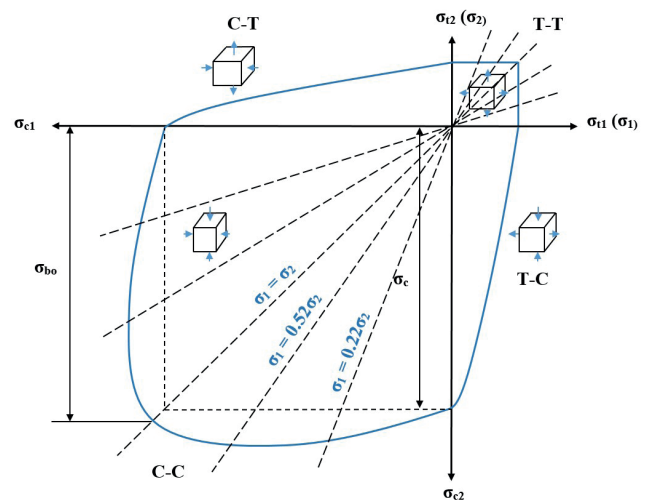

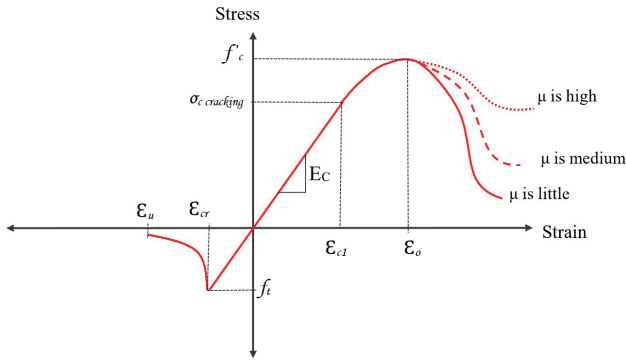**Fig. 4** Failure surface by Kupfer and Gerstle [10]

Fig. 5 Relationship of stress-strain in compression and tension with viscosity parameter [23]

substance [4, 25]. Fig. 5 illustrates the stress-strain relationship in compression and tension. Therefore, this parameter depends on representing the material properties in compression and tension. When the viscosity raises, the regression portion, which describes the softening in compression strain, becomes shallower than the softening when viscosity decreases [26]. Four values are adopted in this study to clarify their effect on the beam behavior.

3 The Practically implemented beam

The practical model of reinforced UHPC beam adopted in this study was accomplished by Yang et al. [27]. The beam had a (180 × 270) mm cross-section and 2900 mm length with a clear span of 2700 mm, as illustrated in Fig. 6. It was reinforced by 3–13 mm tensile steel rebars without stirrups. The shear span to depth (a/d) ratio was 4.8. Practically, the beam was tested for flexure. The compressive strength of UHPC was 193 MPa, and the tensile strength was 25 MPa. The first crack in the compression stress-strain relationship is assumed at 30% compressive strength, and the tensile cracking occurs at the tensile strength. Regarding the tested beam, the first crack appeared at 69.5 kN with a corresponding deflection of 2.04 mm. The sustained peak load was 172.6 kN with a corresponding deflection of 15.14 mm.

4 Calibration of CDP model parameters for the practical beam

The beam was numerically simulated by Abaqus CAE in this study, as shown in Fig. 7. Material properties of UHPC and steel rebar used in defining the CDP model are illustrated in Table 1. The contact between supporting and loading steel plates and the concrete was surface to surface of two types of behavior; tangential contact with penalty friction formulation having 0.5 friction coefficient [14, 28], besides normal behavior with hard contact to prevent the

penetration between the adjacent surfaces. The steel plates were constrained as a rigid body. The rebars were constrained as an embedded region inside the host region of the concrete beam. UHPC beam, steel plates, and rebars were seeded using a 20 mm size mesh, as shown in Fig. 8.
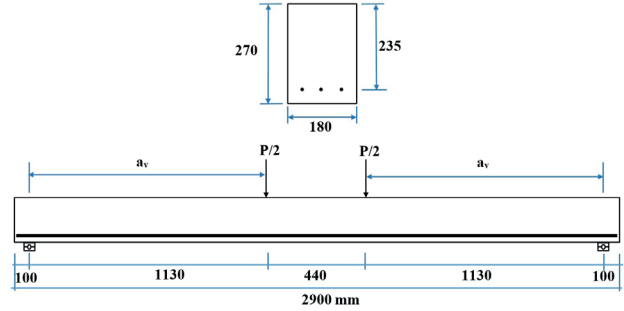

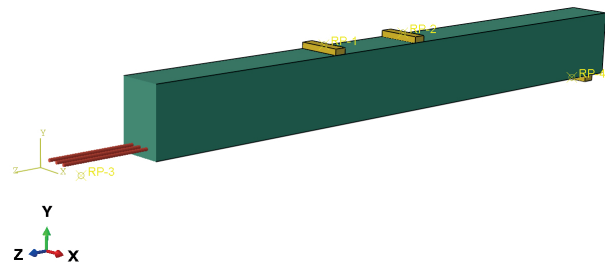**Fig. 6** Practical UHPC beam implemented by Yang et al. [27] adopted in this study

Fig. 7 Numerical simulation of adopted beam by Abaqus

Table 1 Material properties for CDP model definition

Material	Properties
UHPC	f_c' = 193 MPa; ε_u = 0.0035; ε_p = 0.0062; ε_{max}^{in} = 0.00388; E_c = 54320 f_t = 25 MPa; ε_{cr} = 0.00106; ε_{ut} = 0.0112; Poison's ratio = 0.19 ψ = 35°; eccentricity = 0.1; K = 0.667; f_{bo}/f_{co} = 1.16; viscosity parameter = 0.008
Rebar	f_y = 500 MPa; E_s = 200 GPa; ε_y = 0.0025; Poison's ratio = 0.30

Where f_c' and f_t are the UHPC compressive and tensile strength, E_c and E_s are the concrete and steel rebar elastic modulus. ε_u and ε_p are the concrete strain at f_c' and the ultimate state. ε_{cr} and ε_{ut} are the concrete cracking and furthest strain in tension, and f_y and ε_y are the yield stress and strain of steel rebar. ε_{max}^{in} is the inelastic strain in concrete.
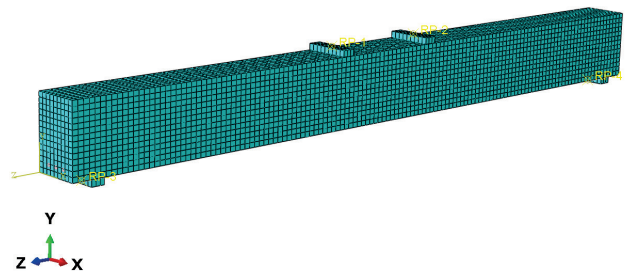

Fig. 8 Meshing of the adopted beam (20 mm mesh size for UHPC beam and rebars)

Supporting steel plates were fixed at the lower region by preventing displacements and rotation in the three directions at the initial step of analysis that propagated at the second step. The loading was due to displacement control using only a downward "y" offset at the reference points in the middle of the loading plates.

5 Results of numerical analysis

The practically implemented beam was modeled by Abaqus CAE. The numerical results were calibrated with the practical results adopting an appropriate model for stress-strain in compressive and tensile behavior of UHPC [29], as shown in Fig. 9. As well as calibration of the five parameters of the CDP model as illustrated in Table 1. The beam calibration was based on matching the sustained loads at the first cracking and the peak state with the deflection approach in both cases.

The load values and deflections from the numerical analysis were very close to the experimental results, as illustrated in Table 2. Where P_{cr} and P_u are the cracking and ultimate load. Δcr and Δu are the cracking strain and the strain at ultimate load.

Modifying parameters' values related to the CDP model and their impact on the structural behavior of the approved beam are explained below.

5.1 Impact of changing shape factor (K)

Three K-values were tested via Abaqus: 0.5, 0.67, and 1.0 to show their effect on the UHPC beam behavior. Modifying the K-value did not affect the first crack load and the corresponding deflection. That behavior is rational because the influence of the shape parameter occurs after failure.

On the peak state, the load capacity was not affected by variation of the K-value, but the deflection slightly decreased upon increasing the K-value from 0.5 to 1.0. Changing K from 0.5 to 0.67 lowered the deflection by only 0.7% while altering it from 0.67 to 1.0 minimized the deflection by about 5%. Therefore, changing the K-value did not significantly affect the loads and deflections at the first crack and peak states, as illustrated in Fig. 10. Furthermore, the analysis period increased when the K-value raised from 0.5 to 1.0. The analysis period at K = 0.67 was about twice the one at K = 0.5. When K = 1.0, the period was approximately six times that at K = 0.5. At K = 1.0, the cracks extended more than that in the case of a 0.5 K-value. This effect was rational due to changing the failure shape from a pyramidal into a triangular base to a conical with a circular base.

5.2 Impact of changing the dilation angle (ψ)

The dilation angle must be greater than zero and less than 56 degrees. Since the dilation angle represents the
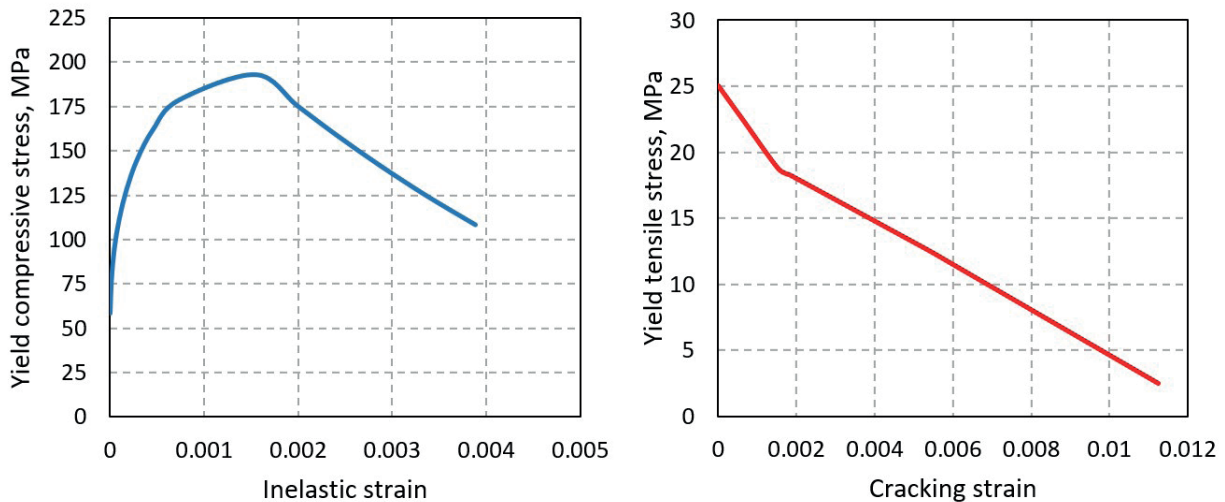

Fig. 9 Compressive and tensile behavior of UHPC after yielding

Table 2 Experimental and FE results of Practical beam

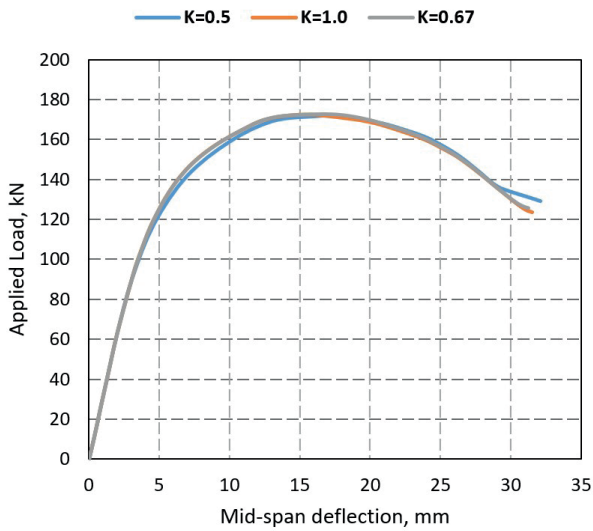| Beam | First crack state | | | | | | Peak state | | | | | |
| | FEA | | EXP [27] | | P_{cr} FEA/EXP | Δcr FEA/EXP | FEA | | EXP [27] | | P_u FEA/EXP | Δu FEA/EXP |
	P_{cr}, kN	Δcr mm	P_{cr}, kN	Δcr mm			P_u, kN	Δu mm	P_u, kN	Δu mm		
UHPC beam	63.17	2.01	69.5	2.04	0.91	0.99	172.6	16.77	172.6	15.24	1.00	1.10

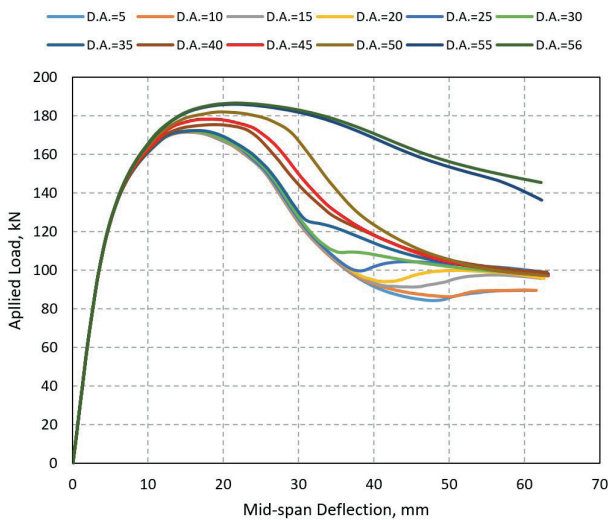**Fig. 10** Effect of shape parameter on Load-deflection relationship of the UHPC beam

Fig. 11 Effect of Dilation Angle on Load-deflection relationship of the UHPC beam

deviation of the concrete element when it undergoes shear to determine the failure surface, it subjects to horizontal and vertical compressive stresses. Therefore, the dilation angle must be greater than zero.

Twelve values of dilation angle are tested for the CDP model, as illustrated in Fig. 11. The dilatation angle was considered to be: 5, 10, 15, 20, 25, 30, 35, 40, 45, 50, and 56. At the first crack stage, there is no effect of the dilation angle on the cracking load and corresponding deflection. It is a sensible result because the influence of variation of dilation angle occurs after failure. At peak state, the impact of the dilation angle on the sustained load can be divided into two parts. When the dilation angle is less than 30°, no effect occurs at peak load and deflection, whereas when

the dilation angle is higher than 30°, increasing the dilation angle raises the peak load and deflection but reduces the time consumed for analysis, as shown in Figs. 12 and 13.

Increasing ψ from 5° to 35° raises the load by only 0.44% and the deflection by 1.42%, whereas increasing it to 56° raises the load by 8.55% and the deflection by 34.5%.

Increasing ψ from 30° to 56° raises the load by 8.25% and the deflection by 33.1%. The percentage of increment in load capacity per every 5° after ψ of 35° is approximately 2%, while the increment of deflection for every 5° after 35° ranges between (3–7.5) %.

Thus, the dilation angle causes more increment in load capacity and deflection after 35° than when it is lower than 30º. This variation in impact is due to the dilation angle being governed by the plastic flow potential that depends on eccentricity and dilation angle, as illustrated in Fig. 14 [17].

5.3 Impact of the ratio of biaxial to uniaxial compressive strength (f_{bo}/f_{co})

Eight values of fbo/bco were tested in the analysis: 0.75, 0.9, 1.0, 1.1, 1.16, 1.18, 1.2, and 1.5. At the first crack state,
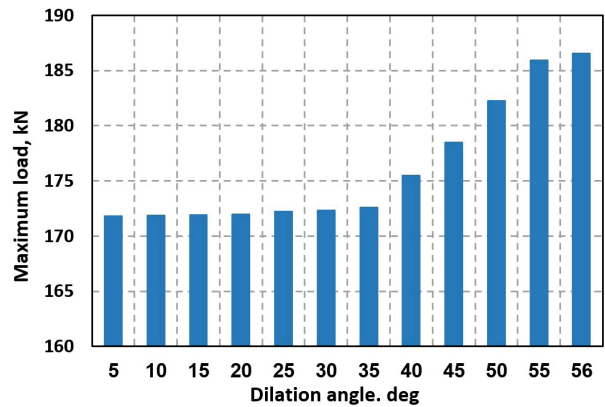

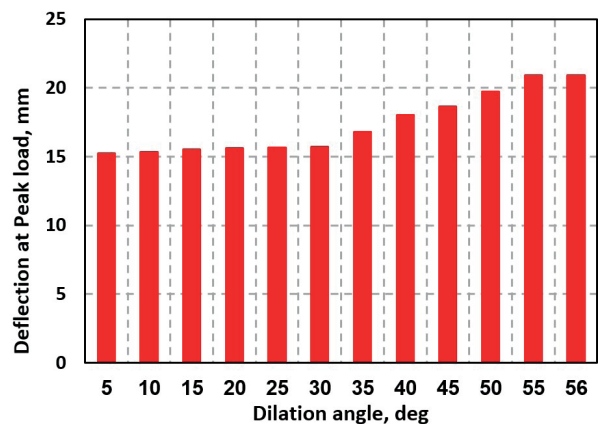**Fig. 12** Effect of variation of dilation angle on maximum sustained load

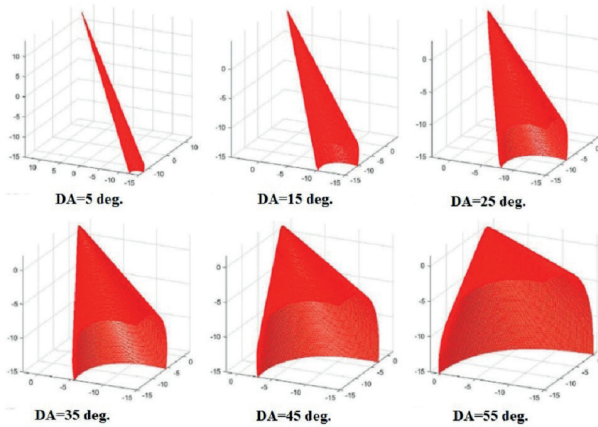**Fig. 13** Effect of variation of dilation angle on deflection at peak load

Fig. 14 Variation of failure surface with the dilation angle [14]

the load and the corresponding deflection were identical for all values of f_{bo}/f_{co}, as shown in Fig. 15, which is a reasonable result due to the variation of f_{bo}/f_{co} parameter impacts after failure. At peak state, the sustained load was identical, while the corresponding deflection was not identical. The highest deflection occurred at $f_{bo}/f_{co} = 1.16$ and 1.20. The lowest deflection occurred when the ratio was 1.5, as shown in Fig. 16.

It can be concluded that the strength of UHPC under biaxial compressive stress is similar to the uniaxial compressive stress, which is unlike the normal strength concrete mentioned by Kupfer. However, the sole effect is related to the beam stiffness that is relied on a deflection. At the first crack state, the induced biaxial stress has the same effect; therefore, no difference in the load carried by the beam or in the deflection.

Abaqus CAE did not analyze the beam when the ratio of f_{bo}/f_{co} was 0.5. The analysis was aborted at the first increment in loading after performing five attempts to catch the equilibrium iteration. That behavior occurred at different time increments. Therefore, the biaxial strength must be greater than half the uniaxial strength subjected to the finite-concrete element.

5.4 Impact of changing eccentricity (ε)
Four values were tested for eccentricity to show its effect on the UHPC beam behavior: 0.0, 0.05, 0.1, and 0.2. It was noticed that changing the eccentricity did not impact the load amplitude registered at the first crack and the peak state. It also did not affect the deflections recorded at the mentioned loads, as illustrated in Fig. 17. The crack pattern and propagation were similar in the four cases.

The lack of eccentricity effect on the UHPC beam may be due to the relatively high tensile strength since the crack initiation depends on the tensile strength, which was
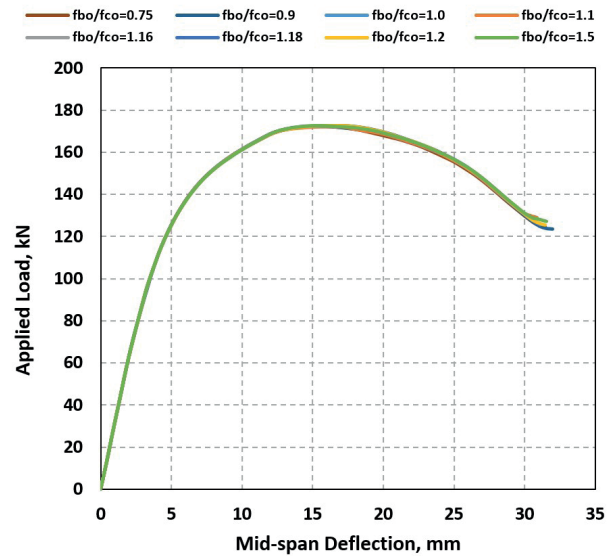

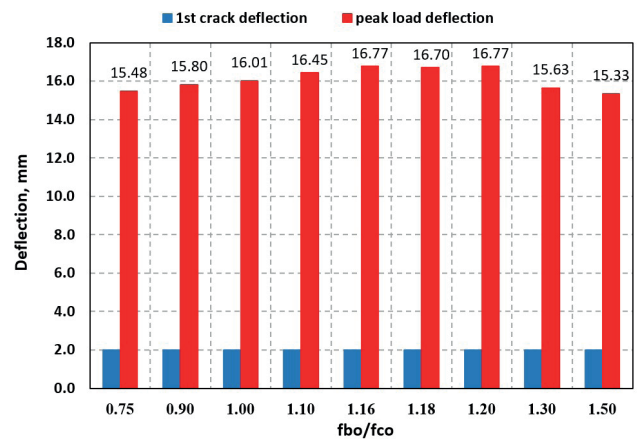**Fig. 15** Effect of f_{bo}/f_{co} parameter on Load-deflection relationship of the UHPC beam

Fig. 16 Effect of f_{bo}/f_{co} parameter on deflection of UHPC beam
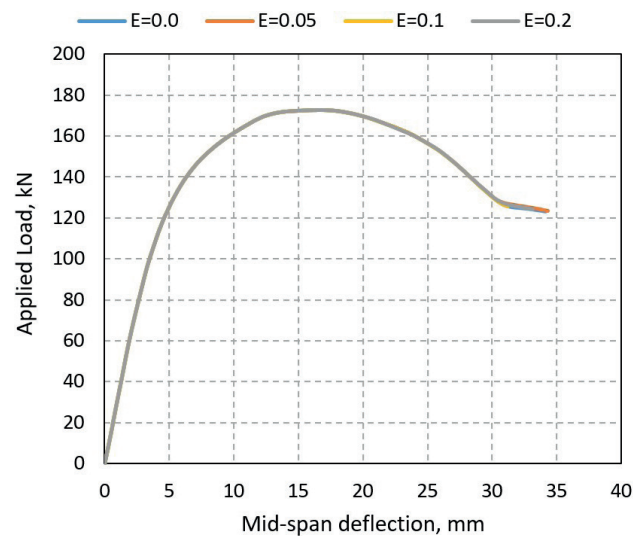

Fig. 17 Effect of Eccentricity parameter on Load-deflection relationship of the UHPC beam

25 MPa for the UHPC. Also, the high compressive strength affects the lack of the eccentricity impact where the first crack was assumed at 30% of compressive strength, which was 193 MPa.

5.5 Impact of Changing the Viscosity Parameter

Automatic incrementing was applied in a static-general analysis step with an initial increment of 0.001, minimum increment of 1e-35, and maximum increment of 0.05. These values were used to capture the first analysis step with an initial increment due to the iteration method adopted by Abaqus and to minimize the increment time in the subsequent steps to modify the stiffness shape matrix. Therefore, when using a viscosity value of zero, the analysis aborted after several time increments. This analysis abort occurred because the material behavior turned into a nonlinear behavior due to crack initiation. Thus, the lowest viscosity used in this study was 0.0001 and increased to be: 0.001, 0.005, 0.008, 0.01, 0.03, and the highest value was 0.05.

At the first cracking state, viscosity variation did not affect the load capacity and deflection. At peak state, increasing the viscosity raised the load capacity and deflection, as shown in Fig. 18. Increasing the viscosity from 0.0001 to 0.001, 0.008, and 0.05 raised the load by 7%, 31%, and 128%, respectively, and the deflection by 22%, 61%, and 129%, respectively, as illustrated in Figs. 19 and 20.

Those increases were because the behavior of UHPC diverted more ductile when the viscosity increased, which
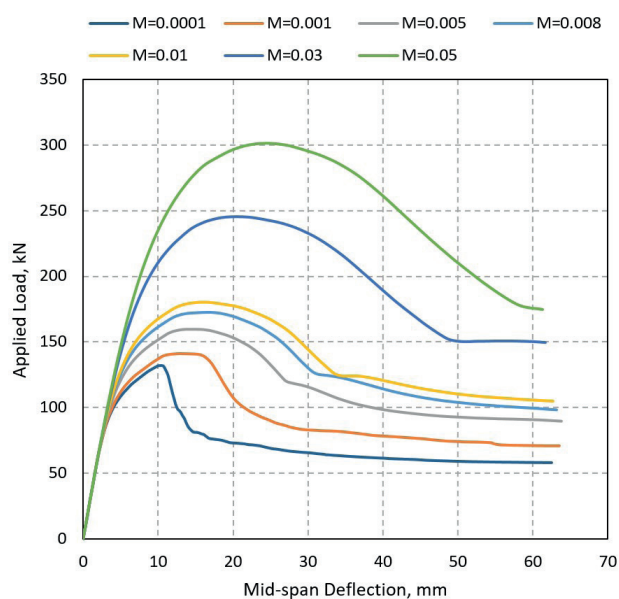

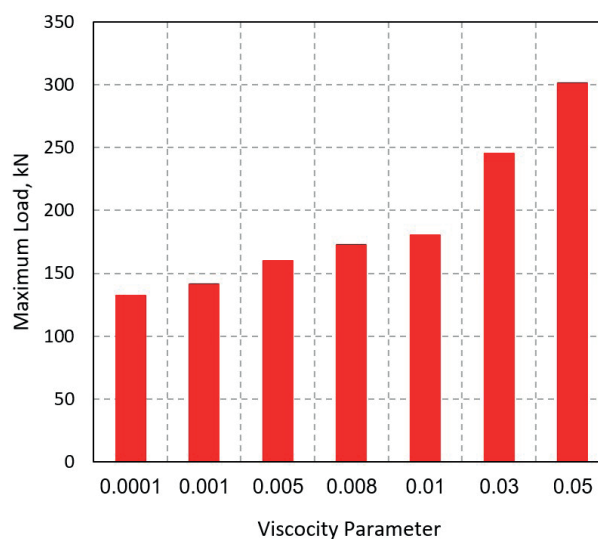**Fig. 18** Effect of Viscosity parameter on Load-deflection relationship of the UHPC beam

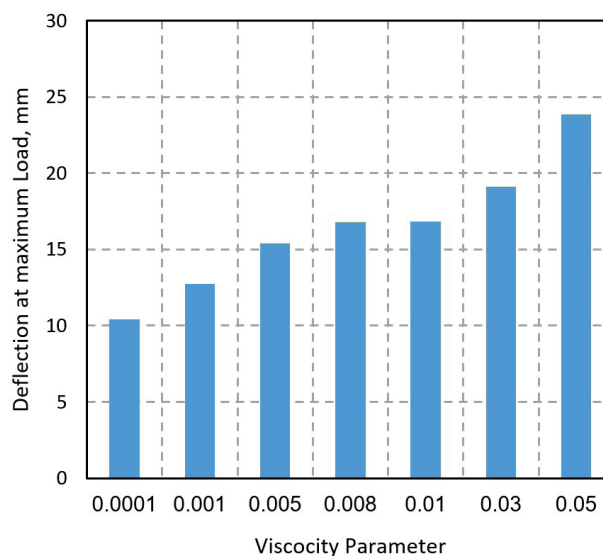**Fig. 19** Effect of viscosity parameter on maximum load

Fig. 20 Effect of viscosity parameter on deflection at peak state

made it bear higher loads and show more deflection. The softening portion of the stress-strain relationship in the case of high viscosity value is shallower than in the case of low viscosity. So, that behavior of the material reflects on beam behavior at loading.

6 Conclusions

This paper introduces numerical analysis for variation of failure surface parameters that can be used for the CDP model in Abaqus software and their effects on the behavior of UHPC beams. The following conclusions can derive:

1. Changing the eccentricity value does not impact the load amplitude and the deflection at the first cracking and the peak states. The crack pattern also does not impact by the change.

2. Changing the shape parameter and the fbo/fco values does not impact the load amplitude and the deflection at the first cracking state. At peak state, the deflection is slightly influenced by changing the shape value. The higher the K-value, the lower the deflection. However, the time consumed for analysis increases when $K = 1.0$ and the cracks extend further. On the other hand, the highest deflection occurs at f_{bo}/f_{co} of 1.16 and 1.20, and the lowest one occurs at $f_{bo}/f_{co} = 1.5$.

3. The biaxial strength must be greater than half the uniaxial strength subjected to the finite-concrete element.

4. The dilation angle must be greater than zero and lower than 56 degrees. At the first cracking state, the variation of the dilation angle does not affect the load capacity and the deflection. At peak state, when the dilation angle is less than 30 degrees, no effect occurs at the load and the deflection. When the dilation angle is more than 30 degrees, increasing it raises the load capacity and the deflection while reducing the analysis time.

5. At the first cracking state, viscosity variation does not affect the load capacity and deflection. At the peak state, increasing viscosity raises the load and the deflection.

References

[1] Sakr, M. A., Osama, B., El Korany, T. M. "Modeling of Ultra-High Performance Fiber Reinforced Concrete Columns under Eccentric Loading", Structures, 32, pp. 2195–210, 2021.
https://doi.org/10.1016/j.istruc.2021.04.026

[2] Kwak, H.-G., Filippou, F. C. "Finite Element Analysis of Reinforced Concrete Structures under Monotonic Loads", Department of Civil Engineering, University of California, Berkeley, CA, USA, Rep. UCB/SEMM-90/14, 1990.

[3] Dassault Systems "ABAQUS Version 6.10-1 Analysis User's Manual", 2017.

[4] Dassault Systems "Abaqus 6.14 / Analysis User's Guide", 2014.

[5] Chen, L., Graybeal, B. A. "Modeling Structural Performance of Ultrahigh Performance Concrete I-Girders", Journal of Bridge Engineering, 17(5), pp. 754–764, 2012.
https://doi.org/10.1061/(asce)be.1943-5592.0000305

[6] Solhmirzaei, R., Kodur, V. "A Numerical Model for Tracing Structural Response of Ultra-High Performance Concrete Beams", Modelling, 2(4), pp. 448–466, 2021.
https://doi.org/10.3390/modelling2040024

[7] Rad, M. M., Ibrahim, S. K., Lógó, J. "Limit design of reinforced concrete haunched beams by the control of the residual plastic deformation", Structures, 39, pp. 987–996, 2022.
https://doi.org/10.1016/j.istruc.2022.03.080

[8] Ibrahim, S. K., Rad, M. M., Habashneh, M. A. "The effects of parameter uncertainties on the numerical plastic analysis of non-prismatic reinforced concrete beams", IOP Conference Series: Materials Science and Engineering, 1141(1), 012038, 2021.
https://doi.org/10.1088/1757-899x/1141/1/012038

[9] Ibrahim, S. K., Rad, M. M. "Numerical Plastic Analysis of Non-Prismatic Reinforced Concrete Beams Strengthened by Carbon Fiber Reinforced Polymers", In: Proceedings of the 13th fib International PhD Symposium in Civil Engineering, Paris, France, 2020, pp. 208–215. ISBN 978-2-940643-06-6

[10] e Silva, L. M., Christoforo, A. L., Carvalho, R. C. "Calibration of Concrete Damaged Plasticity Model Parameters for Shear Walls", Revista Matéria, 26(1), e12944, 2021.
https://doi.org/10.1590/s1517-707620210001.1244

[11] Sümer, Y., Aktaş, M. "Defining Parameters for Concrete Damage Plasticity Model", Challenge Journal of Structural Mechanics, 1(3), pp. 149–155, 2015.
https://doi.org/10.20528/cjsmec.2015.07.023

[12] Jabbar, A. M., Hamood, M. J., Mohammed, D. H. "Ultra High Performance Concrete Preparation Technologies and Factors Affecting the Mechanical Properties: A Review", IOP Conference Series: Materials Science and Engineering, 1058(1), 012029, 2021.
https://doi.org/doi:10.1088/1757-899x/1058/1/012029

[13] Kupfer, H., Hilsdorf, H. K., Rusch, H. "Behavior of concrete under biaxial stresses", American Concrete Institute Journal Proceedings, 66(8), pp. 655–666, 1969.
https://doi.org/10.14359/7388

[14] Dudchenko, A. V., Kuznetsov, S. V. "The Modified Mohr - Coulomb and Drucker - Prager Models. Influence of Eccentricity on Hysteresis Loop and Energy Loss", International Journal for Computational Civil and Structural Engineering, 13, pp. 35–44, 2017.
https://doi.org/doi:10.22337/2587-9618-2017-13-2-35-44

[15] Othman, H., Marzouk, H. "Applicability of Damage Plasticity Constitutive Model for Ultra-High Performance Fibre-Reinforced Concrete under Impact Loads", International Journal of Impact Engineering, 114, pp. 20–31, 2018.
https://doi.org/10.1016/j.ijimpeng.2017.12.013

[16] Altaee, M., Kadhim, M., Altayee, S., Adheem, A. "Employment of Damage Plasticity Constitutive Model for Concrete Members Subjected to High Strain-Rate", In: Proceedings of the 1st International Multi-Disciplinary Conference Theme: Sustainable Development and Smart Planning, IMDC-SDSP 2020, Online Conference, June, 28–30, 2020.
https://doi.org/10.4108/eai.28-6-2020.2298164

[17] Wosatko, A., Winnicki, A, Polak, M. A., Pamin, J. "Role of dilatancy angle in plasticity-based models of concrete", Archives of Civil and Mechanical Engineering, 19(4), pp. 1268–1283, 2019.
https://doi.org/10.1016/j.acme.2019.07.003

[18] Bahij, S., Adekunle, S. K., Al-Osta, M., Ahmad, S., Al-Dulaijan, S. U., Rahman, M. K. "Numerical Investigation of the Shear Behavior of Reinforced Ultra-High-Performance Concrete Beams", Structural Concrete, 19(1), pp. 305–317, 2018.
https://doi.org/10.1002/suco.201700062

[19] Zhang, Y., Xin, H., Correia, J. A. F. O. "Fracture Evaluation of Ultra-High-Performance Fiber Reinforced Concrete (UHPFRC)", Engineering Failure Analysis, 120, 105076, 2021.
https://doi.org/10.1016/j.engfailanal.2020.105076

[20] Rossi, P., Daviau-Desnoyers, D., Tailhan, J.-L. "Probabilistic numerical model of cracking in ultra-high performance fibre reinforced concrete (UHPFRC) beams subjected to shear loading", Cement and Concrete Composite, 90, pp. 119–125, 2018.
https://doi.org/10.1016/j.cemconcomp.2018.03.019

[21] Hashim, D. T., Hejazi, F., Lei, V. Y. "Simplified Constitutive and Damage Plasticity Models for UHPFRC with Different Types of Fiber", International Journal of Concrete Structures and Materials, 14, 45, 2020.
https://doi.org/10.1186/s40069-020-00418-9

[22] Jankowiak, T., Łodygowski, T. "Identification of parameters of concrete damage plasticity constitutive model", Foundations of Civil and Environmental Engineering, 6, pp. 53–69, 2005.

[23] Zhang, Y.-G., Lu, M.-W., Hwang, K.-C. "Nonlinear Finite Element Analysis of Concrete Structures", Zeitschrift Für Angewandte Mathematik Und Physik ZAMP, 44, pp. 537–555, 1993.
https://doi.org/10.1007/BF00953666

[24] Tysmans, T., Wozniak, M., Remy, O., Vantomme, J. "Finite Element Modelling of the Biaxial Behaviour of High-Performance Fibre-Reinforced Cement Composites (HPFRCC) Using Concrete Damaged Plasticity", Finite Elements in Analysis and Design, 100, pp. 47–53, 2015.
https://doi.org/10.1016/j.finel.2015.02.004

[25] Birtel, V., Mark, P. "Parameterized Finite Element Modelling of RC Beam Shear Failure", presented at ABAQUS Users' Conference, Cambridge, MA, USA, May, 23–25, 2006.

[26] Jabbar, A. M., Hamood, M. J., Mohammed, D. H. "Impact of Dilation Angle and Viscosity on the Ultra-High Performance Concrete Behavior in Abaqus", In: 2021 International Conference on Advance of Sustainable Engineering and its Application (ICASEA), Wasit, Iraq, 2021, pp. 125–130. ISBN 978-1-6654-9737-4
https://doi.org/10.1109/ICASEA53739.2021.9733087

[27] Yang, I. H., Joh, C., Kim, B. S. "Structural behavior of ultra-high performance concrete beams subjected to bending", Engineering Structures, 32(11), pp. 3478–3487, 2010.
https://doi.org/10.1016/j.engstruct.2010.07.017

[28] Guo, Q., Chen, Q., Xing, Y., Xu, Y., Zhu, Y. "Experimental Study of Friction Resistance between Steel and Concrete in Prefabricated Composite Beam with High-Strength Frictional Bolt", Advances in Materials Science and Engineering, 2020, 1292513, 2020.
https://doi.org/10.1155/2020/1292513

[29] Jabbar, A. M., Hasan, Q. A., Abdul-Husain, Z. A. "A Theoretical Study to Predict the Flexural Strength of Singly and Doubly Reinforced Ultra-High Performance Concrete Beams", Journal of Engineering Science and Technology Review, 15(2), pp. 91–101, 2022.
https://doi.org/10.25103/jestr.152.13